EXHIBIT B

Programmed Pulsewidth Modulated Waveforms for Electromagnetic Interference Mitigation in DC–DC Converters

Andrew C. Wang and Seth R. Sanders

Abstract—The regular switching action of a pulsewidth modulated (PWM) circuit generates conducted and radiated electromagnetic interference (EMI), and may also generate acoustical disturbances. Programmed pulsewidth modulation techniques have been applied using various methods to control harmonics inherent in switched power circuits. In this paper, a method to generate an optimal programmed switching waveform for a dc-dc converter is presented. This switching waveform is optimized to reduce the amplitude of harmonic peaks in the EMI generated by the converter. Experimental results, a brief discussion of sensitivity, and a practical implementation of a circuit to generate the PWM waveform are given.

I. Introduction

THIS paper investigates methods for reducing unwanted spectral components of circuit waveforms in PWM power conversion circuits. Fig. 1(a) shows a portion of a 50% duty cycle square wave and its spectral components. In many applications, the concentration of power at discrete frequencies is undesirable. For instance, it may be necessary to reduce an annoying audible tone, or an electromagnetic interference (EMI) specification may be satisfied by reducing peak harmonic components, or one might be able to reduce the size and weight of filter elements by reducing peak spectral components.

The main approaches considered in this paper rely on the fact that it is possible to operate a PWM type power circuit with a time-varying switching frequency provided the average duty cycle is not disturbed. We employ a programmed waveform that repeats itself after K cycles. A typical programmed PWM waveform and its spectrum is illustrated in Fig. 1(b). Compared to regular PWM, the programmed PWM has a harmonic spacing that is smaller by a factor of K. The extra available harmonic frequencies are used to spread out the spectral energy of a given circuit waveform.

Section II of the paper reviews the main techniques considered in the literature. Sections III and IV illustrate the application of these methods in the context of a dc-dc converter. Experimental results are presented in Section V, and their sensitivity to parameter variation is discussed in Section VI. An implementation is given in Section VII.

Manuscript received June 17, 1992; revised April 23, 1993. This work was supported by Grants from Tandem Computers and the UC Microprogram.

The authors are with the Department of Electrical Engineering and Computer Sciences, University of California, Berkeley, CA 94720.

IEEE Log Number 9211690.

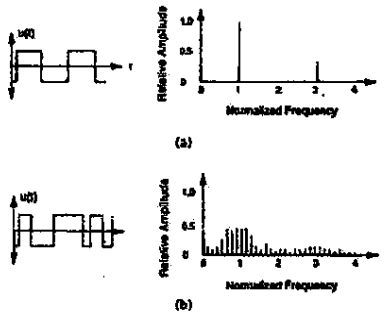

Fig. 1. Typical PWM waveforms and associated spectra. (a) Regular PWM. (b) Programmed PWM.

II. Review of Existing Techniques for Harmonic Control

The first method of harmonic control to be discussed can be termed programmed pulsewidth modulation. In programmed PWM, a precomputed set of turn-on and turn-off times (or angles) is stored in a memory or look-up table, and then accessed periodically by a control circuit. This method can be used to generate steady state waveforms and therefore has found applications in inverters and dc-dc converters. Some of the earliest work in harmonic control is due to Turnbull [1]. In the context of an inverter, Turnbull calculated the necessary turn-on and turn-off angles to generate a modified square-wave that had no third or fifth harmonic components. Waveform symmetry properties, namely quarter-cycle even symmetry and half-cycle odd symmetry, were maintained to assure that no even harmonics were generated. Reference [1] also noted that certain three-phase connections blocked triple-n (i.e., third, sixth, etc.) harmonic components, and that it was advantageous in these three-phase connections to select the switching angles to null the fifth and seventh harmonics. The later work of Patel and Hoft [2],[3] generalized the results of Turnbull by allowing, in principle, an arbitrary number of turn-on and turn-off transitions per cycle. The waveforms in [2],[3] contained the necessary quarter- and half-cycle symmetries to avoid the introduction of even harmonics. Reference [2] applied a Newton-type numerical algorithm to

0885-8993/93$03.00 © 1993 IEEE

determine the switching angles that resulted in a prescribed set of harmonics being nulled. Reference [3] extended the method of [2] to specify the amplitude of the fundamental as well as nulling a given set of harmonic components. The paper [5] of Goodarzi and Hoft took a similar approach to the harmonic control problem, but minimized a weighted square sum of certain harmonic components with the constraint that the amplitude of the fundamental attained a constant value. This method also relied on a Newton-type numerical scheme for determining the optimal switching angles. A summary of the programmed PWM methods is given in the paper [4] of Enjeti *et al.*

A second approach to harmonic control involves randomized switching, and has been quite successfully applied by a number of researchers. It is of interest that with the randomized type switching, one is not restricted to a set of precomputed waveforms. An example of this is the recent work of Tanaka *et al.* [6]. The focus in [6] was not on the lower harmonics of the fundamental switching frequency, but on much higher frequency noise generated by the turn-on and turn-off process in a given dc-dc converter. This work relied on the spectral characterization of the noise generated by each type of transition (turn-on or turn-off), as studied in the authors' earlier papers [7],[8]. Using characterizations of the relevant transitions as impulse responses, the authors were able to deduce the form of the spectrum of a periodic sequence of turn-on and turn-off transitions. Reference [6] then added a random timing component to the switching sequence in an attempt to spread high frequency harmonic components. The random timing component introduced in [6] evidently corresponds to a frequency (or phase) modulation with white noise. The experimental results reported in [6] state that high frequency spectral components are reduced in magnitude by a factor of approximately two or three via the spectral spreading.

A very effective use of randomized switching has been reported in [9]. Reference [9] used a scheme very similar to that of [6] to reduce acoustical and electrical noise harmonics in a PWM induction motor drive. The main difference in [9] with respect to [6] is the use of band-limited modulation. In particular, reference [9] relied on Carson's rule for the estimation of spectral bandwidths in wideband frequency modulation. The result was an effective shaping of the spectrum to reduce harmonic peaks. A reduction of the peak spectral components by a factor of approximately five was obtained. The paper [9] noted that the randomized switching could be implemented by generating the switch times in an on-line manner using a random number generator and shaping filter or by storing a long sequence (a few seconds in length) of switching periods.

Another implementation of randomized switching is in the paper of Legowski *et al.* [10] where a random PWM technique is used to generate a high-quality sine wave inverter output. One apparent drawback of the scheme of [10] is the necessity of increasing the average switching frequency by a large factor. In [14], formulas are presented for estimating the power spectra of several randomized switching schemes. The formulas are verified using Monte-Carlo simulations.

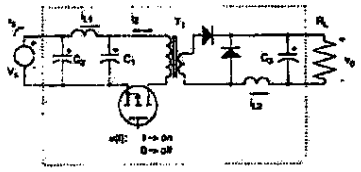

Fig. 2. Forward converter power path frequency, kHz

III. Background

As an example of a circuit where the use of programmed PWM can be compared with regular PWM, we consider the forward converter of Fig. 2. To design a programmed switching sequence for this converter, it is first necessary to choose a circuit waveform that we wish to optimize using the programmed PWM. For example, we may wish to modify the spectrum of the input current $i_s(t)$. Possible criteria can be based on the FCC conducted EMI regulations. Our approach for meeting the FCC regulations is to spread out the spectral energy in $i_s(t)$ to reduce the overall peak amplitude in the spectrum. We accomplish this by first defining a desired spectral envelope for the selected waveform. Then, we apply a constrained min-max optimization algorithm on the switching instants to make the spectrum of the waveform fit under this envelope.

A. Circuit Waveforms

We need to define the programmed PWM waveform, and determine how it affects the waveforms occurring in the converter. For steady-state operation, most of the voltage and current waveforms occurring in the converter can be approximated as filtered versions of the PWM waveform which drives the switch. Some of the waveforms may also contain significant switching transients, which we also consider. Equations for circuit waveforms are given in Section IV.

The programmed PWM waveform is similar to the regular PWM waveform except that the turn-on and turn-off times are varied. Two possible parameterizations for the programmed PWM are given in Fig. 3. In each case, the overall period is multiplied by an integer K so that it contains K subperiods. Subperiod k has length T_k and duty cycle D_k. For the "triangle" parameterization shown in Fig. 3, we require that the "on" time of duration $T_k D_k$ within subperiod k must be centered within this subperiod. Although this restricts the range of admissable PWM waveforms, it is easier to implement in practice using a programmable triangle wave, as will be explained in Section VII. The "sawtooth" parameterization can be used to generate arbitrary PWM waveforms, but requires a programmable sawtooth wave. We have found from optimizations with both parameterizations that the differences in numerical results are not very significant. Therefore, we will limit our discussion below to the triangle parameterization waveform, noting that results obtained with the sawtooth parameterization are similar.

B. Optimization Criteria

The design goal in our experimental work is the suppression of conducted EMI. Conducted EMI onto distribution lines is

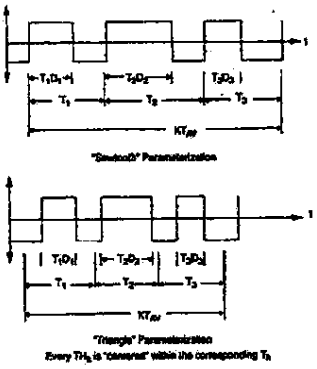

Fig. 3. Possible parameterizations of PWM waveform (for $K = 3$).

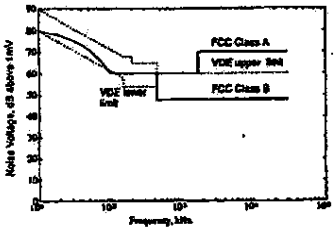

Fig. 4. FCC and VDE conducted EMI limits.

detrimental and therefore regulated by various agencies, such as the FCC and VDE. The noise is generally measured with the use of a line impedance stabilization network (LISN) which presents a specified impedance to the device under test and has a voltage output for noise level measurement. The FCC specified LISN presents an impedance that is almost constant above 1 MHz and that drops off slightly below 1 MHz, as given in [12]. With this LISN, typical FCC conducted noise limits [13] are shown in Fig. 4. Similar VDE regulations are also shown. A reasonable optimization goal in light of these regulations is to reduce the peak harmonic amplitude, weighted by the applicable curve in Fig. 4.

Another possible goal is the reduction of radiated EMI, which is caused by high frequency components ofswitching transients. After implementing appropriate physical layout by elimination of large area current loops, and the use of shielding, a programmed PWM waveform can help spread the spectrum to reduce peak harmonics in the electromagnetic radiation. We could attempt to make the reshaped radiation spectrum fit under the curve of the FCC limits on electromagnetic radiation, shown in Fig. 5.

C. Programmed Waveform Constraints

For our purposes, the programmed PWM waveform must meet several constraints, both in the time and frequency domains.

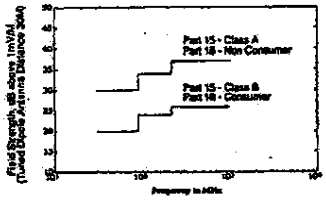

Fig. 5. FCC radiation limits, U.S. code Parts 15 and 18, Title 47.

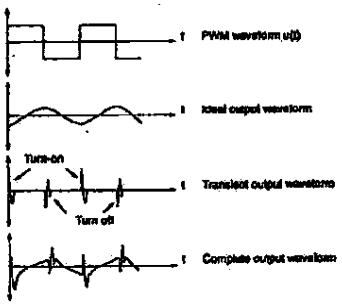

Fig. 6. Output waveform composition.

C1) The programmed PWM waveform must have the same average period and the same average duty cycle as the original PWM waveform.

C2) Every pulse must be longer than some minimal width, due to semiconductor switch constraints.

C3) For control purposes, the average duty cycle of the programmed waveform must be continuously variable via a control signal.

C4) The lowest frequency harmonic in the programmed PWM waveform must be well above the bandwidth f_p of the control loop. Otherwise, the control loop will modify the programmed PWM waveform, even in the steady state.

Constraint ($C4$) limits the maximum number of subperiods in the programmed waveform before it repeats. Let f_o be the original switching frequency, and K be the (integral) number of subperiods in the programmed waveform. Then, K must be less than (f_o/f_p).

IV. Generation of a Programmed Switching Waveform

In this section, we formulate equations necessary for the optimization procedure. We call the waveform that we are trying to optimize (such as the current $i_s(t)$ drawn from the source) the "output waveform" of our optimization. It is the sum of an "ideal" waveform and a "transient" waveform as shown in Fig. 6. The ideal portion of the output waveform is generated by assuming there are no parasitics so that the circuit behaves as if it were ideal. The transient waveform contains only the turn-on and turn-off transient components, which are due to circuit parasitics.

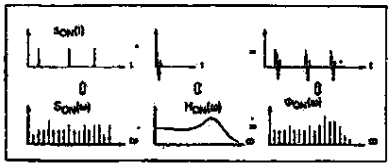

Fig. 7. Calculation of turn-on noise portion of output waveform, and corresponding spectra.

The Fourier series coefficients of the output waveform are denoted $\phi[n]$. In the optimization, we first generate an equation for the relationship between the programmed waveform parameters $(T_1, T_2, \ldots, T_{K-1}, D_1, \ldots, D_{K-1})$ and $\phi[n]$. Next, we weight $\phi[n]$ with a simple function to specify an optimization target for the relative harmonic amplitudes. Finally, the constraints are implemented, and then the optimization performed.

We denote the average length of the subperiods in the programmed PWM by T_{AV}, which must be equal to the period of the original PWM waveform, due to constraint $(C1)$. Similarly, again by $(C1)$, the average duty cycle D_o of the programmed PWM must be the same as that of the regular PWM. In the additional definitions below, functions of time are noted in lower case. Their Fourier series representations are also in lower case, as bracketed functions of n. Fourier transforms are in upper case.

$s_{ON}(t)$	Function containing a unit impulse at each turn-on instant
$s_{OFF}(t)$	Function containing a unit impulse at each turn-on instant
$u(t)$	PWM switching waveform
$H_{ON}(\omega)$	Fourier transform of turn-on transient
$H_{OFF}(\omega)$	Fourier transform of turn-off transient
$\zeta(t)$	Signum function
$H_1(\omega)$	Transfer function from PWM switching waveform to output waveform
$\phi_{ID}[n]$	Fourier series coefficients of ideal output waveform
$\phi_{TR}[n]$	Fourier series coefficients of turn-on and turn-off transient portion of output waveform
$\phi[n]$	Fourier series coefficients of complete output waveform

The period of the programmed PWM waveform is KT_{AV}, therefore, the lowest programmed PWM harmonic occurs at $\omega_0 = (2\pi)/(KT_{AV})$. Due to constraint $(C1)$, the last subperiod and its duty cycle are given by:

$$T_K = KT_{AV} - \sum_{k=1}^{K-1} T_k \tag{1}$$

$$D_L = \frac{KT_{AV}D_0 - \sum_{k=1}^{K-1} T_k D_k}{T_k} \tag{2}$$

We use the functions $s_{ON}(t)$ and $s_{OFF}(t)$ as a starting point for our calculation of the output waveform's Fourier series representation. The functions $s_{ON}(t)$ and $s_{OFF}(t)$ are

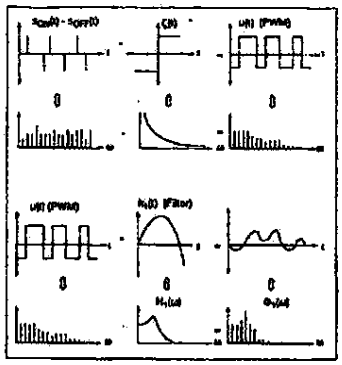

Fig. 8. Calculation of ideal portion of output waveform and corresponding spectra.

defined as waveforms with impulses at the PWM waveform turn-on times and turn-off times, respectively. Hence, they and their corresponding Fourier series representations $s_{ON}[n]$ and $s_{OFF}[n]$ are functions of $T_1, T_2, \ldots, T_K$ and $D_1, D_2, \ldots, D_K$:

$$s_{ON}(t) = \sum_{m=-\infty}^{\infty} \sum_{k=1}^{K} \delta\left(t - \left(T_1 + T_2 + \ldots + \frac{T_k}{2} - \frac{D_k}{2} - mKT_{AV}\right)\right) \tag{3}$$

$$s_{OFF}(t) = \sum_{m=-\infty}^{\infty} \sum_{k=1}^{K} \delta\left(t - \left(T_1 + T_2 + \ldots + \frac{T_k}{2} + \frac{D_k}{2} - mKT_{AV}\right)\right) \tag{4}$$

$$s_{ON}[n] = \sum_{k=1}^{K} e^{\left(-jn\omega_0\left(T_1+T_2+\ldots+\frac{T_k}{2}-\frac{D_k}{2}\right)\right)} \tag{5}$$

$$s_{OFF}[n] = \sum_{k=1}^{K} e^{\left(-jn\omega_0\left(T_1+T_2+\ldots+\frac{T_k}{2}+\frac{D_k}{2}\right)\right)} \tag{6}$$

Now, the Fourier series coefficients $\phi_{TR}[n]$ of a waveform that consists only of the output waveform's turn-on and turn-off transients are easily calculated. We utilize the Fourier transforms of the switching transients in the equations below. An illustration of the calculation for (7) is shown in Fig. 7.

$$\phi_{ON}[n] = s_{ON}[n] \cdot H_{ON}(n\omega_0) \tag{7}$$

$$\phi_{OFF}[n] = s_{OFF}[n] \cdot H_{OFF}(n\omega_0) \tag{8}$$

$$\phi_{TR}[n] = \phi_{ON}[n] + \phi_{OFF}[n] \tag{9}$$

Next, to calculate the Fourier series coefficients $\phi_{ID}[n]$ of the "ideal" portion of the output waveform (without turn-on and turn-off noise), we first generate the PWM waveform $u(t)$ driving the switching element. The ideal output waveform is related to $u(t)$ through a linear, time-invariant (LTI) system, which we characterize by the transfer function $H_1(s)$. The calculation of $\phi_{ID}[n]$ is illustrated in Fig. 8, and equations are

given below:

$$u(t) = (s_{ON}(t) - s_{OFF}(t)) * \zeta(t) \quad (10)$$

$$\phi_{ID}[n] = (s_{ON}[n] - s_{OFF}[n]) \cdot \zeta(n\omega_0) \cdot H_1(n\omega_0) \quad n \in \{1,2,\ldots,\infty\} \quad (11)$$

The Fourier series coefficients of the complete output waveform are obtained in (12), by summing the coefficients of the ideal waveform and the transient waveform. An equivalent form is (13), as required for our optimization algorithm.

$$\phi[n] = \phi_{ID}[n] + \phi_{TR}[n] \quad (12)$$

$$\phi[n] = f_n(T_1, T_2, \ldots, T_{k-1}, D_1, D_2, \ldots, D_{k-1}) \quad (13)$$

To allow for a target spectral envelope that is not flat, we define a weighting function $\Psi[n], n \in \{1,2,\ldots,\infty\}$, where $\Psi[n]$ represents the desired relative amplitude of harmonic n. Then the cost function that we attempt to minimize is (14).

$$J = \max_n\left(\frac{|\phi[n]|}{\Psi[n]}\right) \quad n \in \{1,2,\ldots,\infty\} \quad (14)$$

Thus, the optimization will attempt to make the amplitudes of the harmonicsfit under an "envelope" in the shape described by $\Psi[n]$.

There are some constraints on the domain of the optimization. From constraint (C3), we have the constraint (15), and from constraint (C2), we obtain (16):

$$\begin{matrix} D_k > D_{\min} \\ D_k < D_{\max} \end{matrix} \quad k \in \{1,2,\ldots,K\} \quad (15)$$

$$T_k D_k > T_{\min} \quad k \in \{1,2,\ldots,K\} \quad (16)$$

A. Optimization Method

A suitable algorithm for solving the above constrained min-max problem is available in [11]. It is based on the method of steepest descent, but allows us to find minima of the "max" function given in (14), which is nondifferentiable. The main requirement of the algorithm in [11] is that all the component functions which the maximum is taken over be continuously differentiable over the domain of optimization. This requirement is satisfied except at points where at least one of the harmonic amplitudes is equal to zero. If we start at a point where none of the harmonic amplitudes is equal to zero, the optimization proceeds with no difficulties.

Note that J in (14) is computed on each iteration of the optimization algorithm. We need to limit the number of Fourier coefficients used in the computation of J to make the computation tractable. It has been found that for our conducted EMI calculations, where the lowest frequency harmonics were the largest, using $n \in \{1,2,\ldots,1.25K\}$ allowed the minimization algorithm to converge in a reasonable amount of time for a variety of parameters. All of the results were verified by substituting the resulting optimized T_k and D_k in (14), and checking that the calculated value of J was still valid for large values of n.

Although the min-max algorithm is not guaranteed to find a global minimum, we were able to use it to find useful PWM waveforms. Some optimization weightings gave better results than others in terms of minimizing J, depending on the shape of the weighting. Results are reported in Section V.

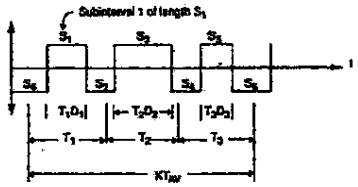

Fig. 9. Definition of subintervals (for K=3).

B. Quantization

In a digital PWM waveform generator, the switching instants of the PWM waveform must be quantized. The step size is equal to the period of the waveform generator's internal clock. For the results in Section V, we used the quantization method described below, which minimizes the largest percentage error in the length of any one "subinterval" of the PWM waveform. A subinterval is defined as the time between two neighboring transitions and is depicted in Fig. 9.

Let $S_m, m \in \{1,2,\ldots,(2K)\}$ be the calculated subinterval lengths and $\bar{S}_m, m \in \{1,2,\ldots,(2K)\}$be the quantized subinterval lengths. Quantization requires that:

$$\bar{S}_m = \frac{P_m}{f_i} \quad (17)$$

where P_m is an integer for $m \in \{1,2,\ldots,(2K)\}$ and f_i is the internal clock frequency of the PWM waveform generator. In our implementation, the constraint on the quantization

$$\sum_{m=1}^{2K} \bar{S}_m = \sum_{m=1}^{2K} S_m \quad (18)$$

was imposed, and the quantization error

$$e = \max_n\left(\left|\frac{\bar{S}_m - S_m}{S_m}\right|\right) \quad m = \{1,2,\ldots,2K\} \quad (19)$$

(19) was minimized. Thus, the largest percentage error in the quantized length of any subinterval was minimized by (19). At the same time, the accuracy of the overall period of the quantized waveform was ensured by (18).

V. Results

For an experimental verification, we used an AT&T model 950A dc-dc forward converter, which is designed for a 48 Vdc input and 5 Vdc output. With a 2.5Ω load, the PWM waveform was a rectangular wave with a 39% duty cycle. To test the programmed PWM, we replaced the gate drive signal in the forward converter with an EPROM based programmable waveform generator. The waveform generator was clocked at 16 MHz, and the programmed PWM transitions occurred only on rising clock edges. In this experiment our interest was in steady-state measurements, and hence the circuit was run open-loop.

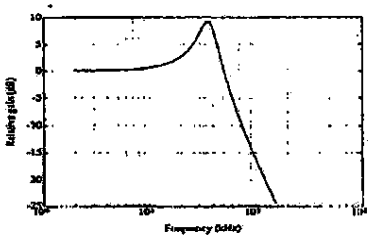

Fig. 10. Transfer function (magnitude) from PWM signal to input current.

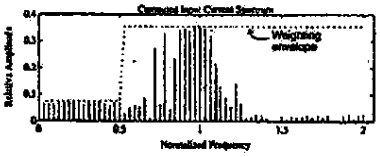

Fig. 11. Optimization result - input current spectrum.

The optimization target was chosen to be the reduction of the amplitude of the largest harmonic in the current waveform drawn by the converter. The essential configuration of the commercial converter's power path, for study of the lower frequency harmonics, is shown in Fig. 2. The relationship between the switching waveform $u(t)$ and the input current $i_1(t)$ in this circuit topology is nonlinear. However, in order to generate the programmed PWM waveform using the process in Section IV, we make the approximation that i_{L2} is constant within each phase of the switch cycle. Then we have:

$$\Phi_1(\omega) = \frac{I_1(\omega)}{U(\omega)} \simeq \frac{I_0}{1 + j\omega R_{L1} C_1 - \omega^2 L_1 C_1} \qquad (20)$$

where R_{L1} is the ac parasitic series resistance associated with L_1 and I_o is a scaling constant. With $L_1 = 6.2uH$, $C_1 = 3.0uF$, and $R_{L1} = 0.1\Omega$ (which is extrapolated from an LC bridge measurement), the magnitude of the transfer function (20) is graphed in Fig. 10.

We found that the input current waveform did not have appreciable switching transients. Therefore, we omitted switching transients from the model used for the optimization.

A. Optimization

The number of subperiods in the programmed PWM waveform to be generated was chosen to be $K = 32$. We set $T_{\min} = 0.1T_{AV}$, $D_{\min} = 0.3$ and $D_{\max} = 0.5$. The spectral weighting was chosen to spread the power of the original first harmonic in the regular PWM to nearby "new" harmonic frequencies in the programmed PWM, and also to minimize the low frequency harmonics in the programmed PWM. It is shown as a dotted line in Fig. 11.

The results of the optimization are also shown in Fig. 11, as vertical bars. Many optimizations were performed with different spectral weightings. In general, attempts at greater suppression of low frequency harmonics caused most of the optimization "effort" to be focused there, and not on making

TABLE I
OPTIMIZATION RESULT — PWM WAVEFORM

h	T	D	h	T	D	h	T	D	h	T	D
1	0.885	0.398	9	0.736	0.413	17	0.665	0.486	25	1.031	0.298
2	0.856	0.389	10	0.848	0.381	18	1.022	0.390	26	0.822	0.389
3	0.842	0.488	11	0.865	0.463	19	1.332	0.282	27	1.085	0.380
4	1.080	0.302	12	1.019	0.368	20	1.020	0.503	28	1.081	0.386
5	1.208	0.306	13	1.056	0.292	21	0.946	0.398	29	1.062	0.389
6	1.264	0.307	14	1.051	0.382	22	0.862	0.398	30	1.021	0.392
7	1.106	0.398	15	0.963	0.486	23	1.323	0.304	31	1.037	0.386
8	0.984	0.389	16	0.864	0.385	24	1.227	0.382	32	0.883	0.486

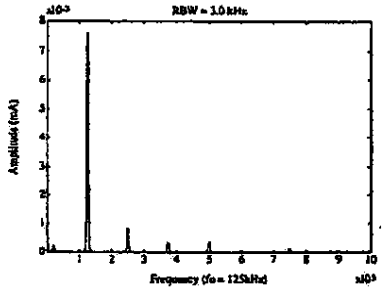

Fig. 12. Measured spectrum of input current, with regular PWM drive (0.001 Hz -1 MHz).

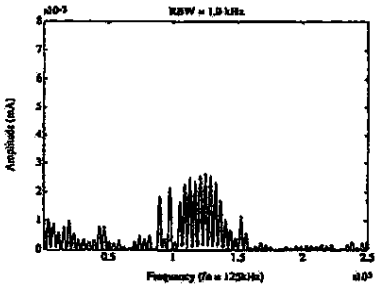

Fig. 13. Measured spectrum of input current, with programmed PWM (0.001 Hz –250 kHz)

the higher frequency harmonics fit the envelope. It was found that relaxing the requirements on the lower harmonics made the upper harmonics fit the target envelope much more closely.

B. Experimental measurements

The target envelope in Fig. 11 produced a good compromise between reduction in size of the largest harmonic and the peak-to-peak amplitude of the ripple, which is larger with programmed PWM than with regular PWM. The waveform generated by the optimization with this target envelope is listed in Table I. Before use in our experiment, the waveform was quantized as described in Section IV-B.

Measurements with the converter began with a regular 39% duty cycle PWM waveform driving the switch at the original switching frequency, f_o = 125 kHz. The spectrum of the resulting input current waveform (as measured by an HP 4195A network/spectrum analyzer) is shown in Fig. 12. With the programmed PWM waveform, the measured spectrum of

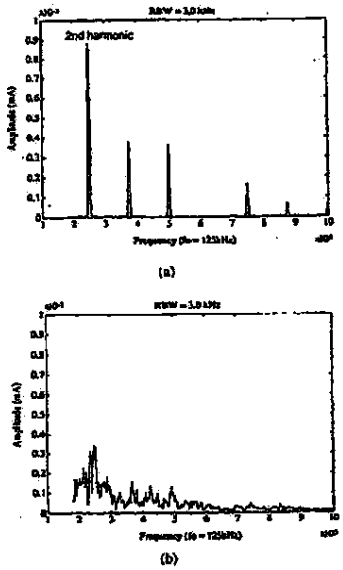

Fig. 14. Measured spectrum of input current, 180 kHz - 1 MHz: (a) Regular PWM. (b) Programmed PWM.

the input current around the original first harmonic became that shown in Fig. 13. Note that the important largest harmonics are very close to those predicted in Fig. 11. Although the lower harmonics are not as well predicted, the power in them is kept very low. The measured peak harmonic amplitude has been reduced from 7.6 to 2.7 mA, or 35% of the original level.

Although the higher frequency harmonics were not considered in the optimization procedure, it is observed that their amplitudes are also reduced by varying degrees and could fit under a smaller envelope. For instance, the amplitude of the second harmonic for regular PWM was 0.85 mA. With programmed PWM, the largest harmonic above 180 kHz is still at 250 kHz, but its amplitude is reduced by 59% to 0.35 mA. Measurements are shown in Fig. 14.

The cost of reducing the size of the peak harmonic includes an increase by 17% of the total power in the harmonics from 1 KHz to 1 MHz. Also, peak-to-peak input current ripple is increased from 28 to 38 mA. In addition, low frequency harmonics are now present, but must be kept above the control circuit's bandwidth for the "optimized" PWM to work.

The results obtained with programmed PWM compare favorably with those reported in [6] for randomized PWM. In [6], it was found that a 15% random deviation in the switching frequency approximately halved the peak level in a converter's switching noise amplitude spectrum (as measured by a spectrum analyzer).

C. Additional optimization results

We have also found that fixing all the D_k's to be equal to the average duty cycle and allowing the optimization algorithm to vary only the T_k's still gave good results, at least in our setup. In fact, with the same parameters as in Section 5.1, but with all of the D_k's fixed at 0.39, the optimization generated a slightly *lower* value of J in (14). The result is shown in Fig. 15, and can be compared to Fig. 11.

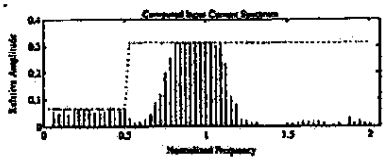

Fig. 15. Optimization result for Dk=0.39, $k \in \{1,2,\ldots,K\}$.

This improved result occurred in spite of the additional constraints becausethe optimization algorithm finds local, but not necessarily global minima. Obviously, in Section V-A, a local minima was found. Therefore, it could be useful to try other starting points for the optimization algorithm in order to find better local minima. One might also try other optimization algorithms such as simulated annealing [15].

VI. Sensitivity

Variations in the switching instants of the actual programmed PWM waveform can cause the spectrum of the output waveform to deviate from the design. The effect of variations on an optimized programmed PWM system are more difficult to analyze than on a circuit using regular PWM. This is mainly due to the fact that the cost index in the optimization is described by a nonlinear "max" function, as seen in (14). A particular harmonic's sensitivity to parameter variations at any point can be found from the partial derivative matrix. However, a highly sensitive harmonic may not be a problem, if the weighted amplitude of the harmonic is much lower than that of the largest harmonic. To get some idea of the sensitivity in light of this difficulty, we consider specific types of parameter variations.

A. Sensitivity to quantization

One type of PWM waveform error may be caused by quantization of the switching instants, or imprecision in the actual circuit. As an example to study, we use the numerical results of Section V. Let the actual values generated by the implementation be called $\overline{D}_k, \overline{T}_k, k \in \{1,2,\ldots,K\}$. Assume each of the $\overline{D}_k$ and $\overline{T}_k$are perturbed from their calculated values by a small percentage:

$$\overline{D}_k = D_k(1+\zeta_k) \quad \overline{T}_k = T_k(1+\eta_k) \qquad k \in \{1,2,\ldots,K\} \tag{21}$$

where the ζ_k's and the η_k's are uniformly distributed random variables between -0.01 and +0.01. It was found that this type of perturbation in the PWM waveform increased one of more of the lower frequency harmonics by a large amount. Fig. 16

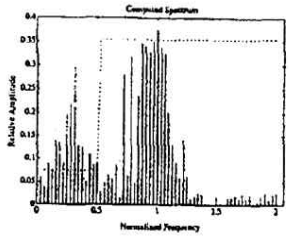

Fig. 16. Programmed PWM spectrum after random perturbation of switching instants.

shows a typical spectrum created by perturbing the results of Section V.

The lower frequency harmonics are affected relatively more than the higher frequency harmonics, mainly due to their nominally small amplitudes. The lower frequency harmonics are nominally small because the target shape of output waveform spectrum was chosen to suppress lower order harmonics. The PWM waveform must have very small low frequency harmonics because it passes through a low pass filter to generate the output waveform, and the low pass filter does little to attenuate these harmonics.

B. Sensitivity to steady-state variations in duty cycle

Another possible deviation in the steady state PWM waveform can be a steady-state deviation in the average duty cycle. An analog control input, which is required for proper regulation, can cause such a deviation. It is impractical to store digital waveform data for all possible average duty cycles. Therefore, Section VII describes an implementation that allows the PWM waveform's average duty cycle to be linearly controlled via an analog control signal. This control signal can cause a change in the output waveform's steady-state spectral distribution.

Control of the average duty cycle with the implementation of Section VII is achieved by adding a fixed amount to each D_k. Let ΔD_{AV} be the change in the average duty cycle that is commanded by the analog control input. Let $\overline{D}_k, k \in \{1, 2, \ldots, K\}$ be the perturbed values of the D_k. $k \in 1.2..., k$ generated by the implementation. The PWM waveform generated by the implementation in Section VII is then described by

$$\overline{D}_k = D_k + \Delta D_{AV}. \tag{22}$$

and the previously computed T_k's.

Again, we look at how the results from Section V would be affected. For reference, the spectrum of the original 39% average duty cycle waveform is shown in Fig. 17(b). Fig. 17(a) shows the result of perturbing the calculated 39% duty cycle waveform to a 29% average duty cycle, while Fig. 17(c) is for a perturbation to a 49% duty cycle. Note that the perturbation in the PWM waveform is much greater here than in Section VI-A, but the shape of the spectrum is not affected very much at all.

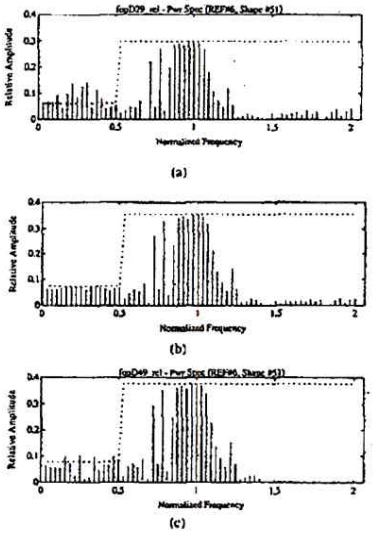

Fig. 17. Computed spectrum of output waveform when (a) average duty cycle is perturbed to 29%. (b) Average duty cycle is not perturbed (39%). (c) Average duty cycle is perturbed to 49%.

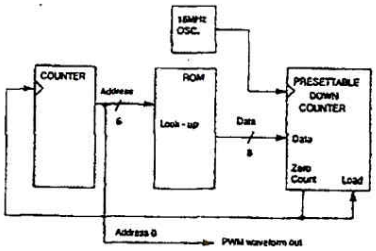

Fig. 18. Simplified PWM generator used in Section V for open-loop measurements.

VII. Implementation

The experimental circuit of Section V was run for open-loop testing only, with the PWM waveform generator depicted in Fig. 18. It lacks an analog section and therefore the duty cycle control input required for feedback control. For a 32 subperiod sequence, 64 bytes of EPROM are required.

A full implementation of the programmed waveform generator with a continuous control input can be based on a programmable triangle waveform generator. Two numbers are stored for every subperiod. One controls the slope of the triangle waveform, and therefore, the length of the subperiod. The other is added to the control signal, and therefore changes the duty ratio of a given subperiod from the average. The

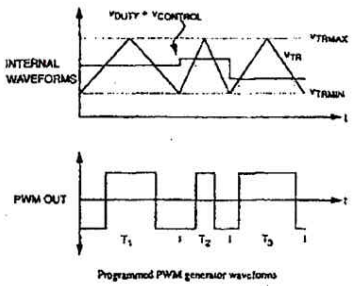

Fig. 19. Programmed PWM generator waveforms

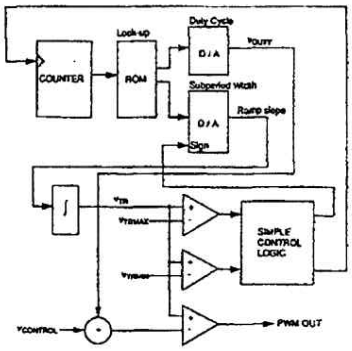

Fig. 20. Programmed PWM generator implementation with control input.

important waveforms and the resulting programmed PWM output are shown in Fig. 19. A block diagram implementation is shown in Fig. 20. Note that the average duty cycle can be varied linearly with the standard duty ratio control signal, marked $v_{CONTROL}$ in Fig. 19. However, the linear range is smaller than with regular PWM in this implementation because of the variation in the D_k's. For the experimental result in Section V, the D_k's only varied from 0.38 to 0.41, so this limitation is not necessarily significant.

VIII. Conclusion

The use of programmed PWM to reduce the magnitude of the peak harmonic in various dc-dc converter circuit waveforms was investigated. A set of equations for the power supply waveforms was presented, along with an optimization method. We found significant reduction possible with a variety of spectral weightings. In the experimental set-up, a reduction in the power of the peak harmonic to approximately one-ninth was achieved in a commercial power converter's input current waveform. Even better results may be possible with other optimization methods, such as simulated annealing.

We also noted that even if we did not allow the D_k's to vary, a reasonable output waveform spectrum could still be achieved, at least in our experimental case. Fixing the D_k's can have additional benefits: the implementation would be simpler and cheaper. Also, the implementation could almost definitely produce a more precise PWM waveform. This would lead to smaller perturbations due to round-off in the switching instants, which cause the output waveform spectrum to change.

Additionally, we found that the spectrum of the input current waveform did not change much when the average duty cycle of the PWM waveform was altered by an analog control input. This is a very useful result for implementation since it implies that only a few optimized waveforms with different average duty cycles need to be stored in ROM.

The relatively large sensitivity of the spectrum to random perturbations (such as round-off) in the switching instants can cause difficulties. However, the quantization technique used in Section V produced experimental results that were very close to the predicted results. Also, choosing the target spectral shape to suppress lower order harmonics can help to prevent them from becoming too large when the PWM waveform is perturbed.

References

[1] F.G. Turnbull, "Selected harmonic reduction in static dc-ac inverters," *IEEE Trans. Commun. Electron.*, vol. 83, pp. 374–378, July 1964.
[2] H.S. Patel and R.G. Hoft, "Generalized techniques of harmonic elimination and voltage control in thyristor inverters: Part I—Harmonic elimination," *IEEE Trans. Industry Applicat.*, vol. IA-9, pp. 310–317, May/June 1973.
[3] ———, "Generalized techniques of harmonic elimination and voltage control in thyristor inverters: Part II— Voltage control techniques," *IEEE Trans. Industry Applicat.*, vol. IA-10, pp. 666–673, Sept./Oct. 1974.
[4] P.N. Enjeti, P.D. Ziogas, and J.F. Lindsay, "Programmed PWM techniques to eliminate harmonics: a critical evaluation," in *Conf. Rec.*, IEEE IAS, 1988, pp. 418–430.
[5] G.A. Goodarzi and R.G. Hoft, "GTO Inverter optimal pwm waveforms," in *Conf. Rec.*, IEEE IAS, 1987, pp. 312–316.
[6] Tanaka, T. Ninomiya, and K. Harada, "Random-switching control in dc-to-dc converters," in *Conf. Rec.*, IEEE PESC, 1989, pp. 500–507.
[7] K. Harada and T. Ninomiya, "Noise generation of a switching regulator," *IEEE Trans. Aerospace Electron. Syst.*, vol. AES-14, pp. 178–184, Jan. 1978.
[8] T. Ninomiya, M. Nakahara, H. Tajima, and K. Harada, "Backward noise generation in forward converters," *IEEE Trans. Power Electron.*, vol. PE-2, pp. 208–216, July 1987.
[9] T.G. Habetler and D.M. Divan, "Acoustic noise reduction in sinusoidal PWM drives using a randomly modulated carrier," in *Conf. Rec.*, IEEE PESC, 1989, pp. 665–671.
[10] S. Legowski and A. Trzynadlowski, "Power-mosfet, hypersonic inverter with high-quality output current," in *Conf. Rec.*, IEEE APEC, 1990, pp. 3–7.
[11] E. Polak, "On the mathematical foundations of nondifferentiable optimization in engineering design," *SIAM Review*, vol. 29, pp. 21–89, March 1987.
[12] Federal Communications Commission, "FCC methods of measurement of radio noise emissions from computing devices," FCC/OST MP-4, Dec. 1983.
[13] N. Mohan, T.M. Undeland, and W.P. Robbins, *Power Electronics*, New York: Wiley, 1989, ch. 17, pp. 427–429.
[14] A.M. Stankovic, G.C. Verghese, and R.O. Hinds, "Monte-Carlo verification of power spectrum formulas for random modulation schemes," Third IEEE Workshop on Computers in Power Electron., Berkeley, CA, Aug. 1992.
[15] M. E. Johnson, Ed., "Simulated annealing (SA) & optimization: Modern algorithms with VLSI, optimal design, & missle defense applications," *Amer. J. Mathemat. and Manag. Sci.*, vol. 8, no. 3 and 4, 1988.

Andrew C. Wang received the B.S. degree (summa cum laude) and the M.S. degree in electrical engineering from the University of California, Berkeley, in 1982 and 1992, respectively.

He is currently with Medical Instrument Development Laboratories, Inc. His interests include applied control systems and computer aided tomography.

Seth R. Sanders received the S.B. degree in electrical engineering and physics, and the S.M. and Ph.D. degrees in electrical engineering, all from the Massachusetts Institute of Technology, Cambridge, in 1981, 1985, 1989, respectively.

He then worked as a design engineer at the Honeywell Test Instrument Division, Denver, CO. He is presently an Assistant Professor with the Department of Electrical Engineering and Computer Sciences at the University of California, Berkeley. His research interests are in nonlinear circuits and systems, and particularly in applications to power electronic and electromechanical systems. During the 1992–1993 academic year, he was on industrial leave with National Semiconductor, Santa Clara, CA. He was awarded the NSF Young Investigator Award in 1988.